Supplementary Information:

Mechanism of Hormone Peptide Activation of a GPCR: Angiotensin II activated state of AT_1R initiated by van der Waals Attraction

Running Title: *AngII-Induced Structural Changes Activating AT_1R*

Khuraijam Dhanachandra Singh, Hamiyet Unal, Russell Desnoyer and Sadashiva S. Karnik*

Department of Molecular Cardiology, Lerner Research Institute, Cleveland Clinic, Cleveland, Ohio 44195, United States

*Correspondence: Sadashiva S. Karnik, Lerner Research Institute, Cleveland Clinic, 9500 Euclid Avenue, Cleveland, Ohio 44195, United States of America

karniks@ccf.org

Table S1. Mutagenesis study of residues within the AT_1R orthosteric site. Effect mutations on K_d of AngII and Sar1-Ile8-AngII is represented as fold change.

Mutation	**AngII**	**Sar1-Ile8-AngII**	**Reference**
Y35A	NB		1
Y35F	NB		1
Y35K	NB		1
Y35I	NB		1
N46G	0.40	0.30	2
C76A	-	0.43	6
D74N	0.84	0.46	2
D74E	-	1	10
D74K	-	NB	10
F77A	1.4	0.44	1,2
F77I	-	1.23	6
F77C	-	0.58	6
F77G	-	1.09	6
W84A	NB		1
W84F	NB		1
W84I	NB		1
Y87A	1.2		1
T88A	1.7		1
Y92A	NB		1
S105A	0.9	1.04	1,4,8
A106G	1.33		4
S107A	2.4	1.09	4
V108A	1.4		1,4
S109A	1.0	1.23	1,4,8
F110A	1.5		4
N111G	2.53	0.70	2,6,7
N111W	0.67	0.25	2,6
N111S	-	1.85	7
N111A	-	0.73	7
N111I	-	0.84	7
N111Y	-	1.32	8
N111G/N46G	0.56	0.26	2,6
N111G/D74N	0.59	0.43	2,6
N111W/F77A	1.72	0.61	2,6
N111G/Q257A	-	0.7	9
L112A	2.0		1
Y113F	0.67	0.92	4, 8,9
Y113A	1.7	0.7	4,9
A114G	1.5		4
S115A	1		4
V116A	1.09	0.7	4,9
F117A	1.5		4
C121A	-	0.79	6

C149A	-	0.21	6
A163G	1.0		1
R167A	NB		1
R167K	1.0		1
R167Q	NB		1
F182A	NB	1.17	1,9
F182Y	1.3		1
F182I	1.0		1
Y184A	-	0.70	9
E185D	-	1	10
E185K	-	1	10
E185Q	-	1	10
K199A	NB	0.21	1,9
K199Q	NB	2.52	1,8
K199R	1.1		1
N200A	1.6		1
F208A	-	1.00	9
W253A	1.4	0.32	1,9
H256A	0.8	1.41	1,3,8,9
H256Q		1.41	3
H256I	1.42	0.76	3
Q257A	1.6	2.90	1,8,9
D263A	-	1	10
D263K	-	1	10
D263E	-	1	10
D278A	-	0.08	10
D278K	-	0.01	10
D281A	0.5	0.03	1,5,10
D281E	-	0.04	10
D281K	-	NB	10
N111G/D281A	0.67		5
M284A	0.4		1
P285A	1.3		1
T287A	-	0.54	9
I288A	NB		1
I288F	2.2		1
C289A	-	0.95	6, 7
Y292A	0.6	0.41	1,9
N295A	-	0.11	9
C296A	-	1.0	6
C296G	-	0.54	6
C296I	-	0.69	6
C296F	-	0.77	6
C355A	-	0.74	6
C76A, C296A	-	0.64	6
C76A, C289A	-	1.03	6
C76A, C289A, C296A	-	0.90	6
C76A/F77A	-	0.27	6
F77A, C289A	-	0.90	6

F77A, C296A	-	0.71	6
F77A, C289A, C296A	-	0.77	6
C76A, F77A, C289A	-	0.95	6
C76A, F77A, C296A	-	0.50	6
F77A, N111G	-	2.18	6
N111G, C296A	-	1.16	6
F77A, N111G, C296A	-	0.97	6
A73C, C76A	-	0.09	7
D74C, C76A	-	0.11	7
L75C, C76A	-	0.32	7
C76A	-	0.43	7
C76A, F77C	-	0.58	7
C76A/N111G	-	1.32	7
C76A/N111I	-	0.97	7
A73C, C76A/N111G	-	1.19	7
D74C, C76A/N111G	-	0.48	7
L75C, C76A/N111G	-	0.88	7
C76A, F77C/N111G	-	1.61	7
C76A/C289A	0.92	-	4
C76A/A106C/ C289A	1.00	-	4
C76A/S107C/ C289A	1.00	-	4
C76A/V108C/ C289A	0.80	-	4
C76A/S109C/ C289A	0.92	-	4
C76A/F110C/ C289A	2.00		4
C76A/N111C/ C289A	0.86	-	4
C76A/L112C/ C289A	0.75	-	4
C76A/Y113C/ C289A	0.15	-	4
C76A/A114C/ C289A	0.92	-	4
C76A/S115C/ C289A	0.71	-	4
C76A/V116C/ C289A	1.50	-	4
C76A/F117C/ C289A	2.00	-	4
F77A/N1111G	-	0.91	8
S105A/N111G	-	1.16	8
S109A/N111G	-	0.88	8
N111G/K199Q	-	1.87	8
S105A/S109A/N111G	-	1.49	8
S105A/N111G/K199Q	-	1.81	8
S109A/N111G/K199Q	-	1.45	8
S105A/S109A/N111G/K199Q	-	1.29	8

Figure S1 (A) Structure of AngII showing the residues important for binding and initiation of AT_1R activation. (B) AT_1R protein secondary structure showing residues important for AngII binding (blue) and activation (red).

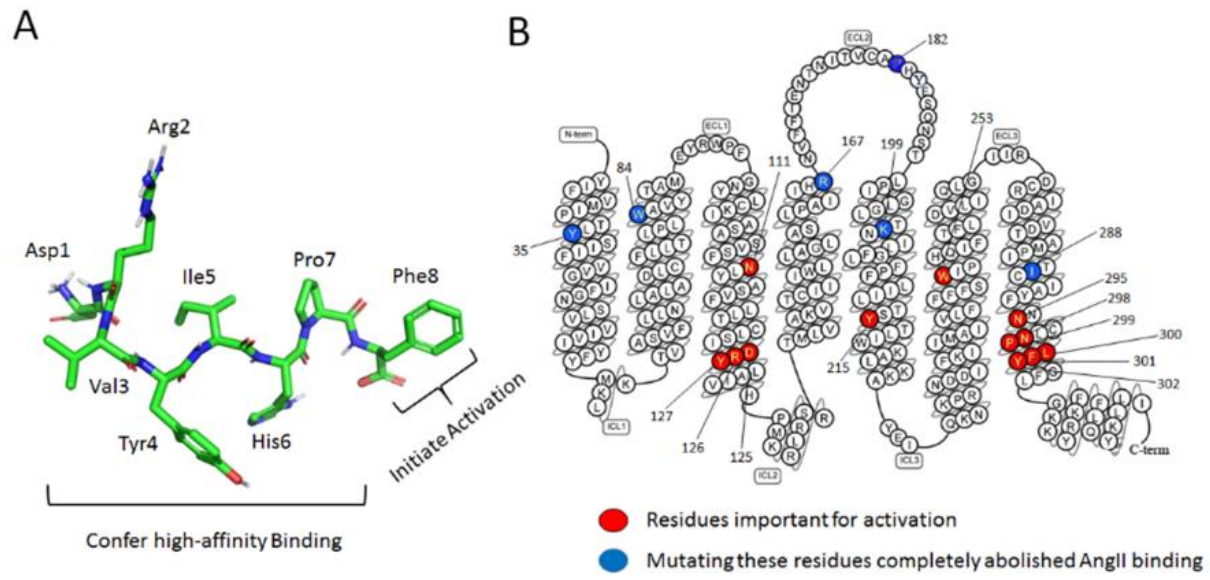

Figure S2. (A) Backbone RMSD of AT_1R bound with AngII and Olmesartan. RMSD reached plateau when the simulation reaches ~ 0.4 µs. (B) Backbone RMSF of AT_1R bound with AngII and Olmesartan. Significant chnages in RMSF was observed in DRY, ECL2 and ICL3 motifs. High fluctuation in these motif may correlate with the activation of the rceptor.

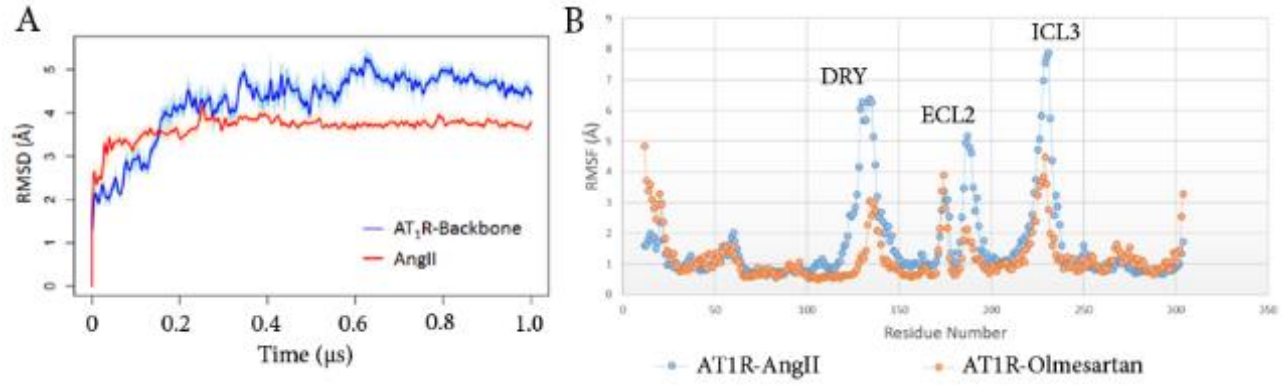

Figure S3. RMSD of TM1-7, H8, ICL3 and ECL2 of AT_1R-AngII (blue) and AT_1R-Olmesartan (red) bound structure.

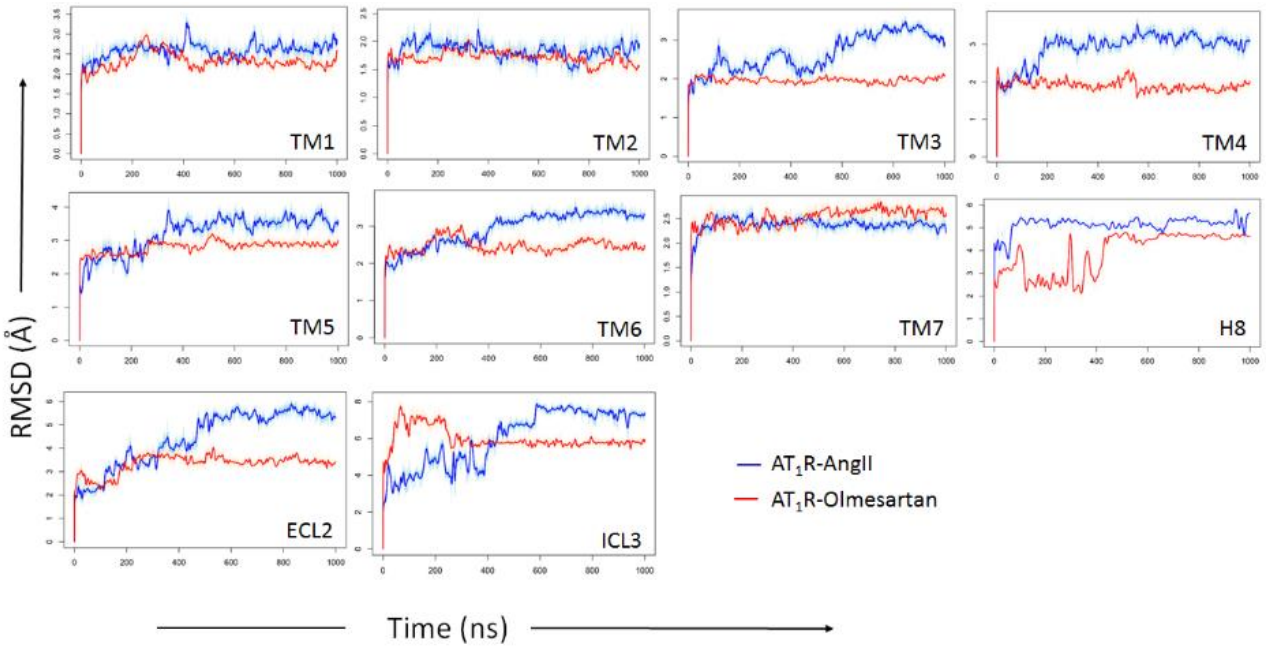

Figure S4. Figure S3. Superimposed TM helixes and loops of AT1R-AngII average structure when it is active like structure using MDS (0.6μs to 1μs) and AT1R-Olmesartan/ZD7155 bound structure (crystal structure). The whole protein structures were superimposed and only the TM-helices are presented for greater view.

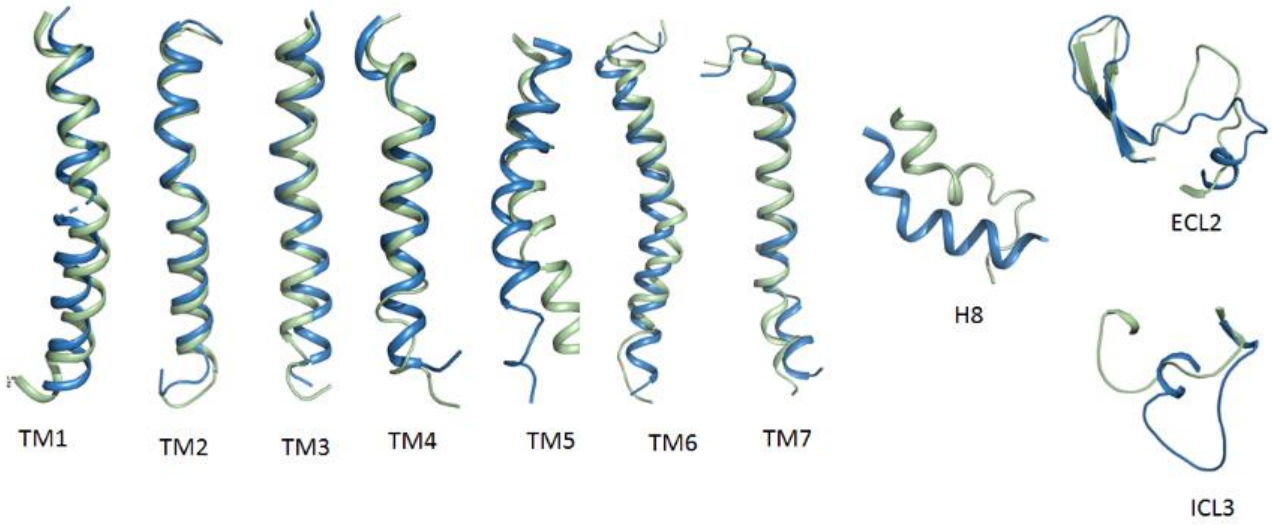

Figure S5. Superimposed binding modes of AngII and Olmesartan. Strong hydrophobic interaction of Phe8AngII with Ile288$^{7.39}$ is competed by stronger hydrophobic interaction of alkyl tail of Olmesartan. This phenomenon is better explained when Phe8^{AngII} is mutated to Ile8^{AngII}, which improves the binding affinity.

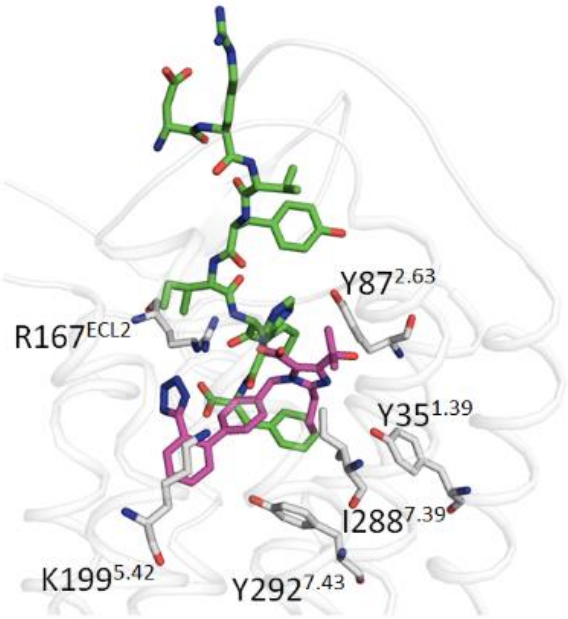

Figure S6. (A) Breakage of V108$^{3.32}$-Y292$^{7.43}$ H-bonding in AngII bound AT_1R in the course of MD simulation. (B) Time scale of bond breakage observed as increase in distance. We also observed a breakage of V108$^{3.32}$-Y292$^{7.43}$ bond in AT_1R-olmesartan bound structure for > 80 ns (780 ns – 850 ns) but there were reformation of bond after 850 ns of MDS. During this breakage of H-bond we also observed breakage of one H-bond in N111$^{3.35}$-N295$^{7.46}$ but one bond was still intact (see Figure S6).

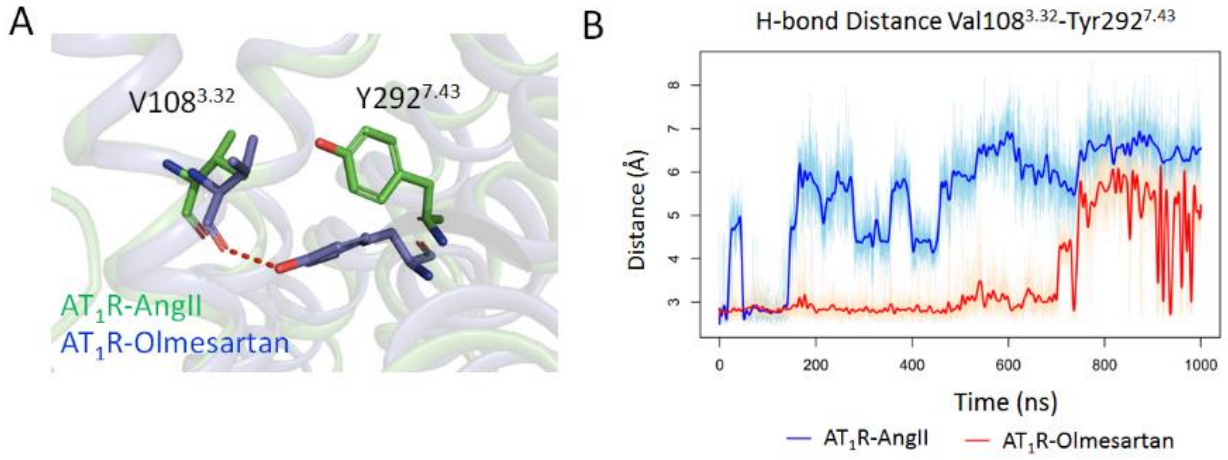

Figure S7. (A) Olmesartan bound AT1R and (B, D) AngII bound AT1R. Time scale of breakage of the first (C) and second (D) H-bonds between $N111^{3.35}$-$N295^{7.46}$ in AngII bound AT1R in the course of MD simulation, observed as increase in distance.

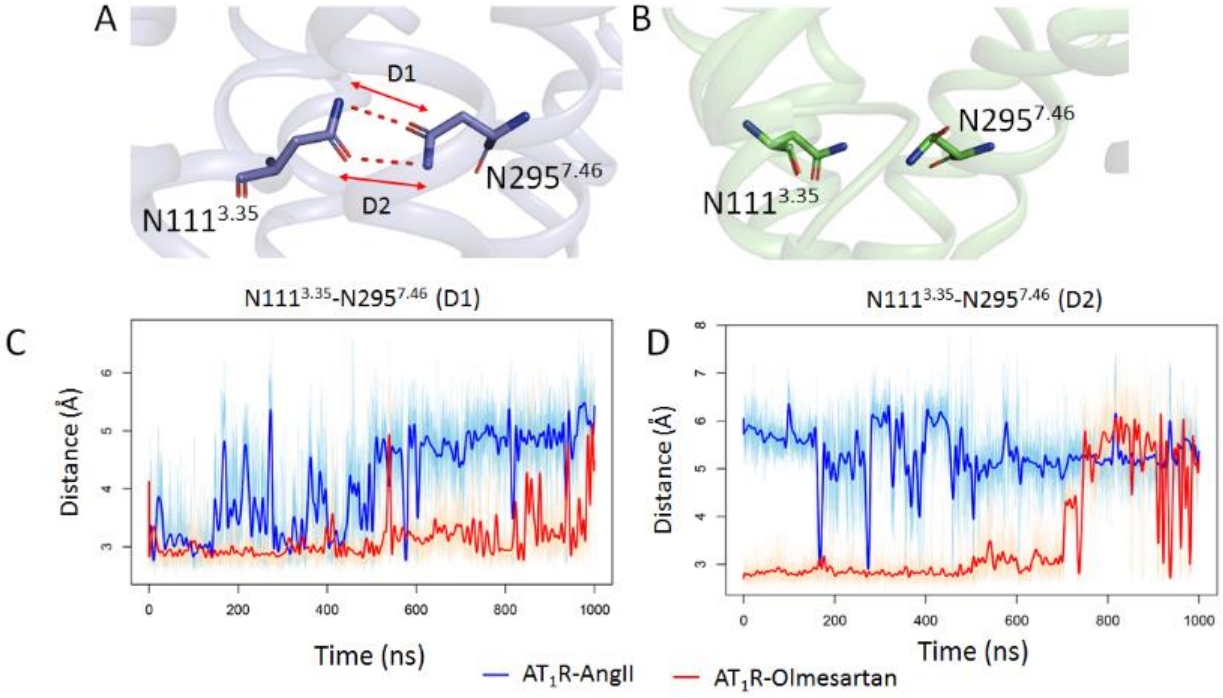

Figure S8. Experimental binding affinity and efficacy data (A). Binding mode of Ile8-AngII (B), Ala8-AngII (C) and Gly8-AngII (D).

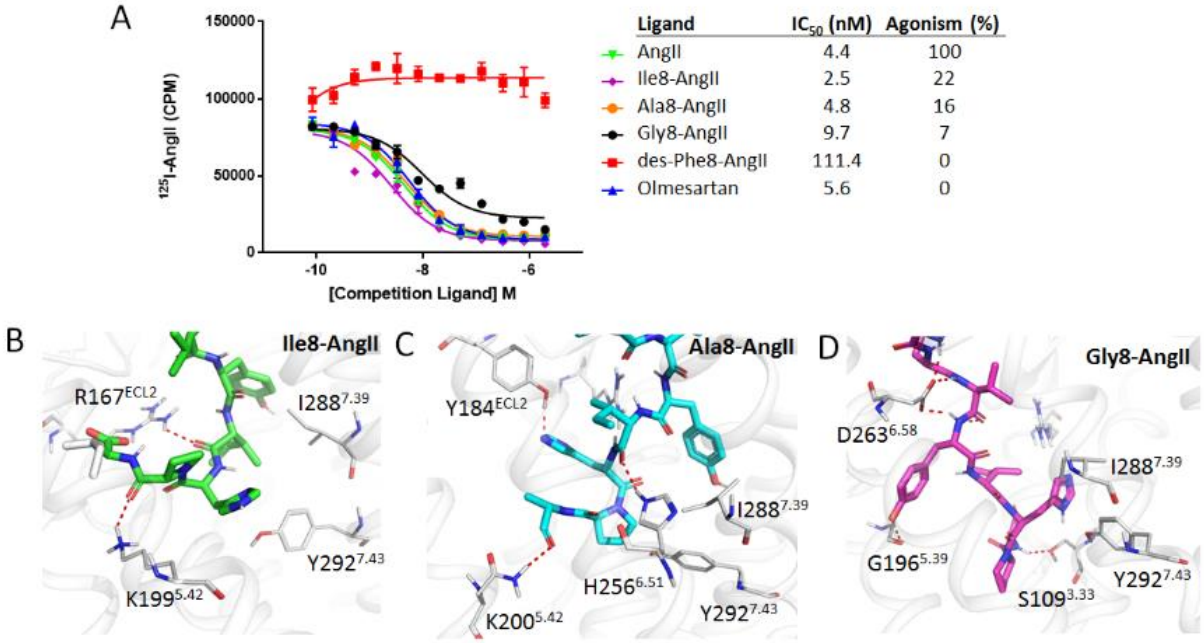

Figure S9. Stick structure shows the important residues in AT_1R which are already reported to be important for its activation. Blue and red highlighted regions are highly conserved hydrophobic region which may be important for transmission of signal from orthosteric site to intracellular region.

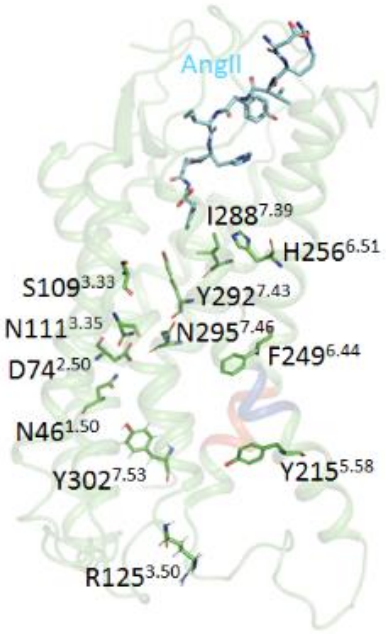

Figure S10. (A) Superimposition of AT_1R-AngII and AT_1R-Olmesartan showing CWxP motif ($W253^{6.48}$). (B) Superimposed structure of $W253^{6.48}$ of AT_1R-AngII with ET_B-Endothelin. (C) Superimposed structure of $W253^{6.48}$ of AT_1R-AngII with A_2AR-Adenosine. (D) Change of Torsion angle of $W253^{6.48}$.

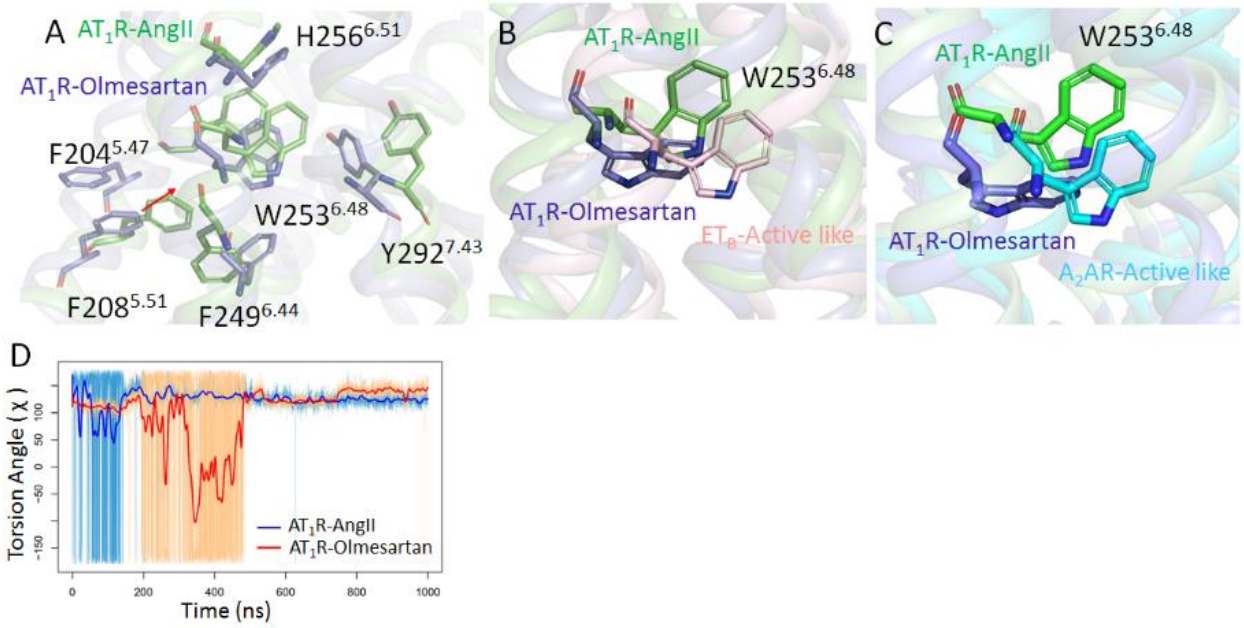

Figure S11. Movement of Tyr215$^{5.58}$ in the AT_1R activation. A-C for AT_1R bound with AngII and D-F for AT_1R bound with Olmesartan.

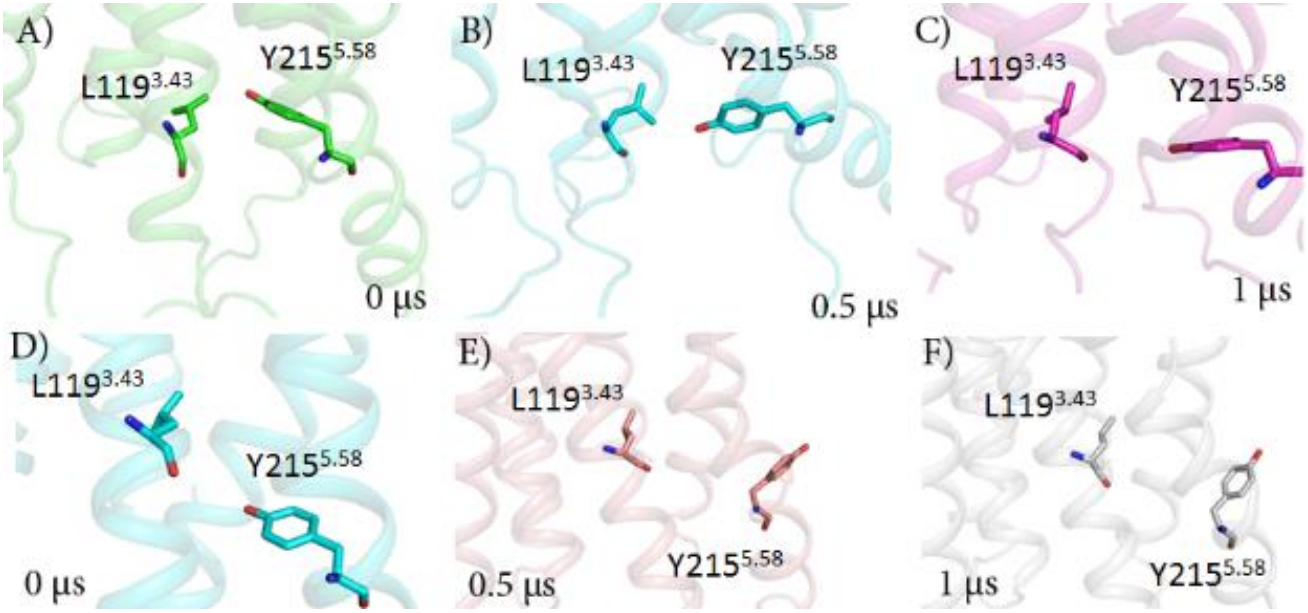

Figure S12. Movement of Arg126$^{3.50}$ in the AT_1R activation. A-C for AT_1R bound with AngII and D-F for AT_1R bound with Olmesartan. R126$^{3.50}$-D237$^{6.32}$ H-bond was observed in AT_1R bound with AngII. This may help an important role in opening of intracellular domain for Gprotein binding.

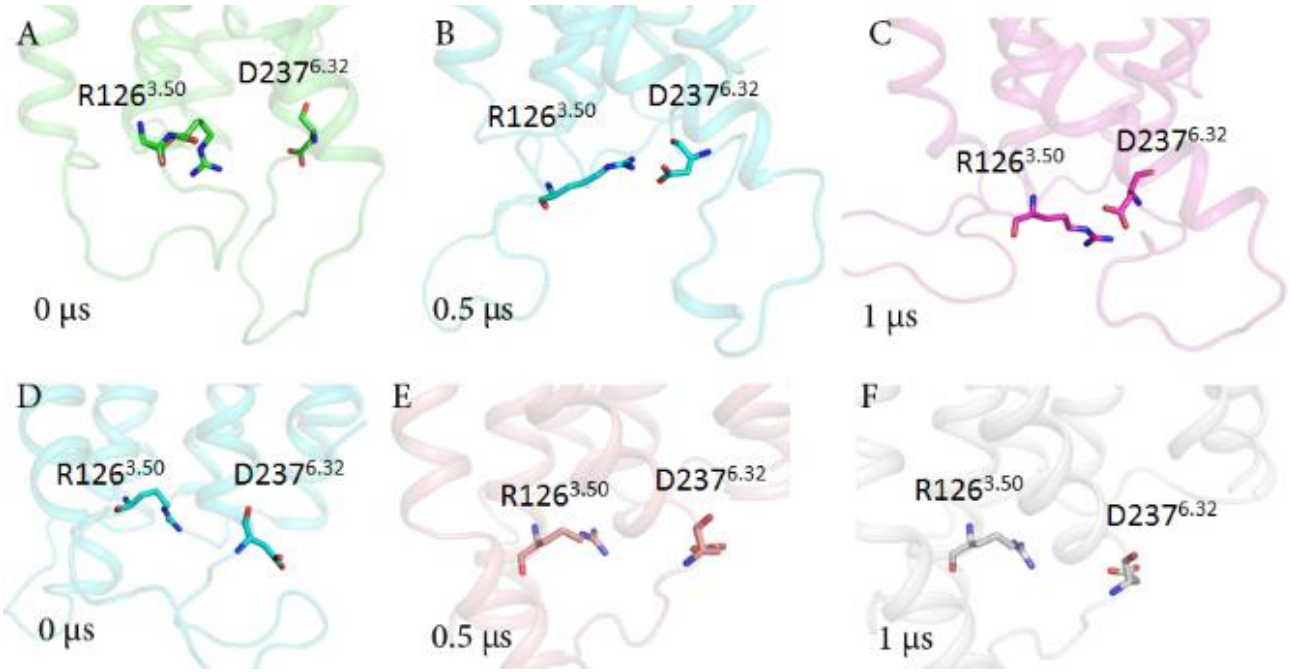

Reference

1. Zhang, H.; Unal, H.; Desnoyer, R.; Han, G. W.; Patel, N.; Katritch, V.; Karnik, S. S.; Cherezov, V.; Stevens, R. C., Structural Basis for Ligand Recognition and Functional Selectivity at Angiotensin Receptor. *J Biol Chem* **2015**, 290, 29127-29139.
2. Cabana, J.; Holleran, B.; Beaulieu, M. E.; Leduc, R.; Escher, E.; Guillemette, G.; Lavigne, P., Critical Hydrogen Bond Formation for Activation of the Angiotensin II Type 1 Receptor. *J Biol Chem* **2013**, 288, 2593-604.
3. Schambye, H. T.; Hjorth, S. A.; Weinstock, J.; Schwartz, T. W., Interaction Between the Nonpeptide Angiotensin Antagonist Skf-108,566 and Histidine 256 (Hisvi:16) of the Angiotensin Type 1 Receptor. *Mol Pharmacol* **1995**, 47, 425-431.
4. Miura, S.; Kiya, Y.; Hanzawa, H.; Nakao, N.; Fujino, M.; Imaizumi, S.; Matsuo, Y.; Yanagisawa, H.; Koike, H.; Komuro, I.; Karnik, S. S.; Saku, K., Small Molecules with Similar Structures Exhibit Agonist, Neutral Antagonist or Inverse Agonist Activity Toward Angiotensin II Type 1 Receptor. *PLoS One* **2013**, 7, e37974.
5. Le, M. T.; Vanderheyden, P. M.; Szaszak, M.; Hunyady, L.; Vauquelin, G., Angiotensin IV is a Potent Agonist for Constitutive Active Human AT1 Receptors. Distinct Roles of the N-and C-terminal Residues of Angiotensin II during AT1 Receptor Activation. *J Biol Chem* **2002**, 277, 23107-23110.
6. Miura, S.; Zhang, J.; Boros, J.; Karnik, S. S., TM2-TM7 Interaction in Coupling Movement of Transmembrane Helices to Activation of the Angiotensin IT Type-1 Receptor. *J Biol Chem* **2003**, 278, 3720-3725.
7. Miura, S.; Karnik, S. S., Constitutive Activation of Angiotensin II Type 1 Receptor Alters the Orientation of Transmembrane Helix-2. *J Biol Chem* **2002**, 277, 24299-24305.
8. Miura, S.; Kiya, Y.; Kanazawa, T.; Imaizumi, S.; Fujino, M.; Matsuo, Y.; Karnik, S. S.; Saku, K., Differential Bonding Interactions of Inverse Agonists of Angiotensin II Type 1 Receptor in Stabilizing the Inactive State. *Mol Endocrinol* **2008**, 22, 139-146.
9. Miura, S.; Okabe, A.; Matsuo, Y.; Karnik, S. S.; Saku, K., Unique Binding Behavior of the Recently Approved Angiotensin II Receptor Blocker Azilsartan Compared with that of Candesartan. *Hypertens Res* **2013**, 36, 134-139.
10. Feng, Y. H.; Noda, K.; Saad, Y.; Liu, X. P.; Husain, A.; Karnik, S. S., The Docking of Arg2 of Angiotensin II with Asp281 of AT1 Receptor is Essential for Full Agonism. *J Biol Chem* **1995**, 270, 12846-12850.